Article

Non-Nucleophilic Electrolyte Based on Ionic Liquid and Magnesium Bis(diisopropyl)amide for Rechargeable Magnesium-Ion Batteries

Lethesh Kallidanthiyil Chellappan,* Jannicke Kvello, Julian Richard Tolchard, Paul Inge Dahl, Sidsel Meli Hanetho, Romain Berthelot, Anne Fiksdahl, and Kaushik Jayasayee*

Read Online

ACCESS | Metrics & More | Article Recommendations | Supporting Information

ABSTRACT: A non-nucleophilic electrolyte for rechargeable Mg-ion batteries is developed by the reaction of magnesium bis(diisopropyl)amide and 1-ethyl-3-methylimidazolium tetrachloroaluminate ionic liquid in tetrahydrofuran solvent. The electrolyte shows excellent reversibility and Coulombic efficiency for the Mg deposition/stripping process at room temperature on several working electrodes such as Mo, graphite, and stainless steel. Additionally, the electrolyte shows high anodic stability with Mo as the cathode current collector, with no corrosion detected even after 48 h at 4.5 V versus (Mg/Mg^{2+}). An exceptional cyclability in a full cell configuration using a Chevrel phase Mo_6S_8 cathode is achieved with a capacity retention of more than 80% for over 300 cycles at a 15 mA g^{-1} specific current, making this electrolyte an excellent candidate for rechargeable Mg-ion batteries.

KEYWORDS: Mg-ion batteries, electrolytes, ionic liquids, magnesium, energy storage
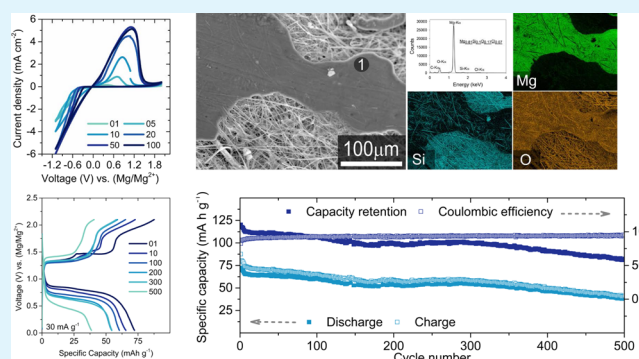
1. INTRODUCTION

The field of Li-ion batteries (LIBs) has shown extraordinary development in the last few decades,[1,2] which has enabled revolutionary changes in portable electronic devices and now underpins a shift away from fossil-fueled transport. However, to satisfy the demand for more capable and versatile energy storage infrastructure, safer, cheaper, and efficient storage technologies alternative to LIBs are necessary. Rechargeable Mg-ion batteries offer many advantages over LIBs[3−6] concerning cost, volumetric capacity, and resistance to dendrite formation that allows the use of metallic Mg as the anode.[7,8] Nevertheless, their success toward commercialization is confronted with compelling challenges on the materials front. Lack of suitable electrolytes with favorable ionic conductivity, the ability to efficiently deposit Mg^{2+} ions reversibly, and a wide electrochemical stability window are some of the most significant challenges to overcome.[9,10]

Ethereal solutions of Grignard-based reagents with a wide range of Mg salts are some of the first known electrolytes for rechargeable Mg-ion batteries with the ability to deposit Mg^{2+} with high Coulombic efficiency (CE) reversibly.[11−13] However, these strongly reducing electrolytes have low ionic conductivity, are highly corrosive, and have poor anodic stability (1.0−2.0 V vs (Mg/Mg^{2+})), restricting them from being used with high voltage cathodes and low-cost collectors.[10,13] The technical feasibility of rechargeable Mg batteries is first reported by Gregory et al. methodically with

intercalation cathodes using THF solutions of organoborates and organohaloaluminates as the electrolytes.[14] The CE and anodic stability of the Grignard-type electrolytes are shown to be improved significantly by the addition of aluminum-based Lewis acids ($AlCl_3$, $AlCl_2BuEt$, etc.) as demonstrated with Mg organohaloaluminate electrolytes such as the first generation "dichloro complex" (DCC) and the second generation "all phenyl complex" (APC).[15,16] Nevertheless, the use of strong Lewis acids makes them reactive with sulfur cathodes and raises safety concerns because of their corrosive and combustible nature.[12,17]

Consequently, the hunt for electrolytes with practical applicability for rechargeable Mg batteries has resulted in a class of electrolytes based on inorganic Mg salts without Grignard reagents.[18−21] Non-nucleophilic electrolytes based on magnesium bis(hexamethyldisilazide), $[Mg(HMDS)_2]$[19,22−24] and borate anion-based electrolytes[25−27] in ethereal solvents have been developed and are shown to have enhanced anodic stability (>3.2 V vs Mg/Mg^{2+}) and CE as well as excellent compatibility with sulfur cathodes. It is essential to mention
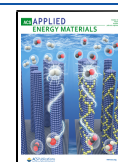
the discovery of reversible Mg deposition/stripping in a nonhalide electrolyte based on the commercial inorganic salt $Mg(BH_4)_2$ in both THF and DME.[28] The low CE and high overpotential for the reversible Mg deposition process in this electrolyte are found to be improved by involving boron clusters such as magnesium monocarborane (MMC) in tetraglyme.[29] Recently, electrolytes based on fluorinated alkoxide and dialkoxide are reported to show reversible Mg deposition/stripping with nearing 100% CE with high anodic stability (>3.0 V vs Mg/Mg^{2+}) on glassy carbon and gold working electrodes.[30,31]

Most of the magnesium electrolytes contain organometallic magnesium complexes, which are highly hazardous and corrosive. These issues are averted in inorganic electrolyte solutions based on the reaction of $MgCl_2$ and $AlCl_3$ in THF, known as magnesium aluminum chloride complexes (MACC) .[18,32] The cationic species in these electrolytes are THF-solvated $MgCl^+$ and $Mg_2Cl_3^+$ in association with an AlC_4^- anion. The MACC electrolytes are reported to exhibit anodic stability of up to 3.4 V versus Mg/Mg^{2+} with Pt and glassy carbon working electrodes. However, preconditioning of MACC electrolytes is necessary to get the required performance as these electrolytes do not contain any active organometallic components to scavenge reducible contaminants.[33,34] More extensive discussions on the evolution of electrolytes for rechargeable Mg batteries can be found in these review papers.[35,36]

Ionic liquids (ILs) exhibit several desirable properties, including wide electrochemical window, high thermal stability, compatibility with a variety of cathode materials, and low vapor pressure. For these reasons, they are extensively investigated as electrolytes for rechargeable Mg-ion batteries.[37−41] In combination with Grignard reagents, ILs in tetrahydrofuran (THF) are found to support the reversible Mg deposition/stripping process, but they are not superior compared to other electrolytes discussed earlier in terms of CE.[42] For instance, a solution of $Mg(BH_4)_2$ in ammonium-based ILs has shown reversible deposition of Mg in the presence of an organic solvent dimethoxyethane (DME).[43] These electrolytes are reductively unstable on Mg metal anodes, which limit their application in a battery with an Mg anode. Alkoxy-functionalized ILs are also reported as electrolytes for rechargeable Mg-ion batteries, but they suffer from low CE for the reversible Mg deposition/stripping process.[43−45]

Recently, a magnesium bis(diisopropyl) amide-aluminum chloride ($Mg(DIPA)_2$-$AlCl_3$) electrolyte developed for Mg−S batteries is reported to show excellent anodic stability using a stainless steel collector.[46] There are also reports revealing the potential for chloride-rich electrolytes based on 1-ethyl-3-methylimidazolium tetrachloroaluminate ($[C_2mim][AlCl_4]$) and $MgCl_2$.[47,48] Nevertheless, insertion and extraction of Mg in a full cell configuration with a proper cathode are not achieved so far with this electrolyte system. Moreover, $[C_2mim][AlCl_4]$ is either used in either acidic or alkaline electrolytes so far, which are corrosive.[49,50]

In this study, we report a novel electrolyte synthesized by simple mixing of commercially available $[C_2mim][AlCl_4]$ with non-nucleophilic $[Mg(DIPA)_2]$ in THF. To the best of our knowledge, this is the first report of a $Mg(DIPA)_2$-based non-nucleophilic Mg salt in combination with chloroaluminate anion-based ILs as an electrolyte for rechargeable Mg-ion batteries. The neutral species of the chloroaluminate ILs used in this study makes this electrolyte less corrosive for the

current collectors at high anodic potentials, which opens up the possibility to work with high-voltage cathodes.[49]

2. EXPERIMENTAL SECTION

2.1. Electrolyte Preparation. All the electrolytes are prepared in an argon-filled glove box with oxygen and water contents of less than 0.1 ppm. The following chemicals from Sigma-Aldrich are used without any further purification; $[Mg(DIPA)_2]$ (0.7 M solution in THF), $[C_2mim][AlCl_4]$ (99.9%), and THF (anhydrous, 99.9%). The electrolyte with a 1:2 molar ratio is prepared by adding a solution of 1 M $[Mg(DIPA)_2]$ to 2 M ($[C_2mim][AlCl_4]$), which is followed by the addition of anhydrous THF (2.5 mL) and stirring at ambient conditions for 24 h. The electrolytes with 2:1 and 1:1 molar ratios are prepared through the same procedure.

2.2. Physical and Chemical Characterization of Materials. The electrolytes are characterized by high-resolution mass spectrometry (HRMS) in positive and negative modes using a "Synapt G2-S" Q-TOF instrument equipped with Waters MassLynx software for spectral data processing. No chromatographic separation is used before the mass analysis. Raman measurements are conducted using a Renishaw InVia Reflex microscope with a 785 laser line.

The electrodes and current collectors are characterized by scanning electron microscopy (SEM) using a Hitachi S-3400 N. X-ray diffraction (XRD) patterns are collected using a Bruker D8 Advance A25 equipped with a Mo Kα source and focusing Gøbel mirror, operating in the θ-θ configuration. Phases are identified via reference to the ICDD PDF4 + .

2.3. Electrochemical Characterization. Cyclic voltammetry (CV) and linear sweep voltammetry (LSV) are performed using a three-electrode T-cell configuration with graphite foil, stainless steel 316 (SS), and molybdenum as working electrodes. The working electrodes are chosen based on literature reports of their potential application as cathode current collectors.[51,52] Metallic Mg discs and Mg strips were used as counter and reference electrodes, respectively. Both the graphite foil and the metal sheets are of 0.5 mm thickness, 10 mm diameter, >99.9% in purity, and are procured from Goodfellow. Before cell assembly inside an argon-filled glove box, the metal pieces used are polished using SiC grinding paper (P800 grit size) and repeatedly washed with dry THF. Cyclic voltammograms are recorded between −1.1 to 2.0 V versus (Mg/Mg^{2+}) with a scan rate of 50 mV s^{-1} to determine the Mg deposition/stripping behavior and CE. Meanwhile, the electrochemical potential window of the electrolyte is measured through LSV from 2.0 to 5.0 V versus (Mg/Mg^{2+}) with a scan rate of 20 mV s^{-1} on different working electrodes. Chronoamperometry measurements are carried out by holding the working electrodes at 3.5 V and 4.5 V versus (Mg/Mg^{2+}) for 48 hours to deteremine the longterm anodic stability. A VMP3 potentiostat from Biologic Instruments is used to investigate the electrochemical properties of the electrolyte.

The electrochemical performance of the electrolyte in full cell configuration is carried out in CR2016 coin cells. Mo_6S_8, synthesized according to the procedure reported in the literature, is used as the active cathode material.[53] The cathode slurry is initially formed by milling Mo_6S_8 with Ketjenblack EC300J carbon and polyvinylidene fluoride (PVDF) in 80:10:10 weight ratio, with N-methyl-2-pyrrolidone (NMP) and acetone (1:10 weight ratio) as solvents. Circular cathodes of 16 mm diameter are prepared on both molybdenum and graphite foil current collectors by drop coating the slurry onto the respective substrates. The coated substrates are dried overnight at 120 °C under vacuum to obtain an active material loading of approximately 2 mg cm^{-2}. The coin cells are assembled inside an argon-filled glove box with polished Mg metal as the anode and a glass microfiber (Whatman GF/D) separator. Galvanostatic discharge/charge cycling is performed using a BCS-805 battery cycler from Biologic Instruments.

3. RESULTS AND DISCUSSION

The electrochemical performance of electrolytes could be tailored by varying the ratios of the ILs and the concentrations

of Mg salt in the ILs. The cyclic voltammograms of Mg deposition/stripping behavior of the $[Mg(DIPA)_2]$ and $([C_2mim][AlCl_4])$ electrolyte in three different molar ratios; 2:1, 1:1, and 1:2, respectively are shown in Figure 1a.
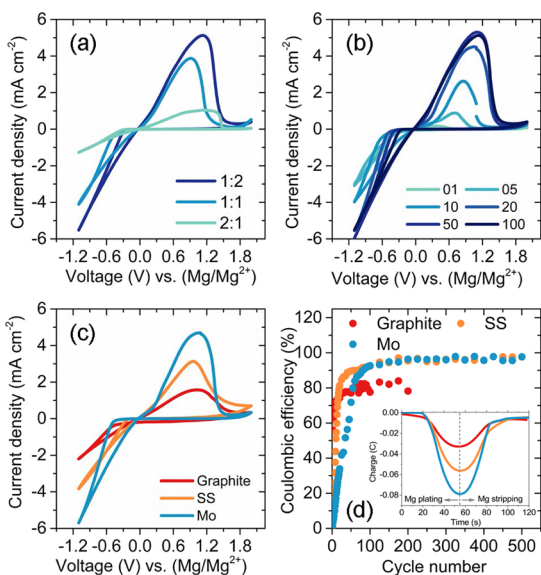

Figure 1. (a) CVs showing Mg deposition/stripping in the IL-based electrolyte with different ratios of $Mg[(DIPA)_2]$-$[C_2mim][AlCl_4]$ using a Mo working electrode recorded at a scan rate of 50 mV s^{-1}. (b) CVs showing the reversibility of the Mg deposition/stripping process for 100 cycles in the 1:2 $Mg[(DIPA)_2]$-$[C_2mim][AlCl_4]$ electrolyte using a Mo working electrode recorded at a scan rate of 50 mV s^{-1}. (c) CVs showing Mg deposition/stripping in the 1:2 $Mg[(DIPA)_2]$-$[C_2mim][AlCl_4]$ electrolyte using different working electrodes recorded at a scan rate of 50 mV s^{-1}. (d) Coulombic efficiencies of the extended reversible Mg deposition/stripping process with different working electrodes evaluated from CVs using the 1:2 $Mg[(DIPA)_2]$-$[C_2mim][AlCl_4]$ electrolyte, and the inset shows the plot of charge over time from the 100th CV scan

Reversible Mg deposition/stripping is achieved on a Mo substrate with all the three electrolyte compositions. The observed CV profiles are typical for Mg dissolution and electrodeposition, with the oxidation current between 0 and 1.6 V versus (Mg/Mg^{2+}) representing Mg dissolution and the reduction current between 0 and −1.1 V versus (Mg/Mg^{2+}) corresponding to Mg electrodeposition. The overpotential and the CE are, however, found to vary with the relative concentrations of the dissolved complexes in THF, with the 1:2 ratio between $Mg[(DIPA)_2]$-$[C_2mim][AlCl_4]$ being the most efficient.

The mechanism for the formation of the electrolyte with a 1:2 ratio of $Mg[(DIPA)_2]$-$[C_2mim][AlCl_4]$ is proposed in Scheme 1. Initially, upon mixing, two types of positively and negatively charged ions are formed in the electrolyte. It has been reported that bis(amide)-based Mg salt, in combination with Lewis acids such as $AlCl_3$, tend to form a positively charged ion (3) and negatively charged ion (5).[50] ESI-MS analysis in the negative ion mode shows a strong peak at m/z = 233.5231 (Figure S1), which corresponds to the presence of aluminum species (5) in the electrolyte. Similarly, the existence of the $[C_2mim]$ cation in the electrolyte is concluded by the presence of molecular ion peak at m/z = 111.0918 (Figure S2) when investigated in the positive ion mode. However, no signals for the chloride anion are observed, which could be due

Scheme 1. Preparation of the Electrolyte Based on $[Mg(DIPA)_2]$-$[C_2mim][AlCl_4]$. (1) Magnesium bis(diisopropyl)amide, (2) 1-Ethyl-3-methylimidazolium Tetrachloroaluminate, (3) $[(\mu\text{-}Cl)_3Mg_2(THF)_6]^+$ Dimer, (4) Chloride Anion, (5) Trichloro-isopropyl Amide Aluminate Complex, (6) 1-Ethyl-3-methylimidazolium Cation
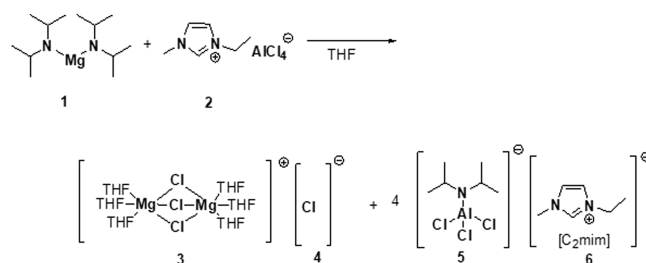
to their low molecular mass, making it undetectable in the mass spectrometer. The molecular ion peak corresponds to the Mg complex, $[Mg_2(\mu\text{-}Cl)_3(THF)_6]^+$, which is also not observed in the ESI-MS analysis. The interaction between Mg and THF is very weak, and it would not survive the harsh operating conditions of ESI-MS with an inlet temperature of more than 200 °C.[54] Nevertheless, there is no conclusive evidence for the association of the ions in the order, as shown in Scheme 1.

Raman spectroscopic studies performed on the electrolyte to identify $[Mg_2(\mu\text{-}Cl)_3(THF)_6]^+$ yielded an unresolved spectrum initially due to strong fluorescence interferences from the solvent molecules, which is in accordance with the earlier reported studies.[54] However, the spectra (Figure S3) obtained from the solidified electrolyte after removing the THF solvent that shows a characteristic peak at around 242 cm^{-1} corresponds to $MgCl_3^+$ in the $[Mg_2(\mu\text{-}Cl)_3(THF)_6]^+$ complex.[33,55] Besides, the characteristic peak of $AlCl_4^-$ is observed at 311 cm^{-1}. However, the peak for its dimer $Al_2Cl_7^-$ (347 cm^{-1}) is not observed in the electrolyte.[56] The bands observed at around 1087, 847, and 739 cm^{-1} belong to the ring asymmetric bending/stretching vibrations in the $[C_4mim]$ ring from the ionic liquids.[57]

The evolution of the Mg deposition/stripping process on the Mo working electrode using the electrolyte with a 1:2 ratio is shown in Figure 1b. The performance of the electrolyte concerning the CE, overpotential, and current density for the Mg stripping/deposition process improves significantly with the cycle number. For instance, the overpotential, which is the difference between the onset potentials of Mg electroplating and stripping on the Mo working electrode improved significantly from 375 mV in the first cycle to 225 mV at the 100th cycle. The overpotential derived from the CVs at 0.2 mA cm^{-2} for the Mg stripping/deposition process on the Mo working electrode remained stable for at least 500 CV cycles, as shown in Figure S4. A similar trend in the overpotential is also found on the graphite and SS working electrodes (Figure S5).

The reversibility for the Mg stripping/deposition process (Figure 1c) and the evolution of the CE over extended cycling (Figure 1d) in the IL-based electrolyte with a 1:2 ratio is investigated through CVs using graphite foil, SS, and Mo working electrodes. Figure 1c demonstrates good reversibility for the Mg stripping/deposition process in all the three working electrodes in general. The CEs on different working electrodes are obtained from the plots of charge over time, as
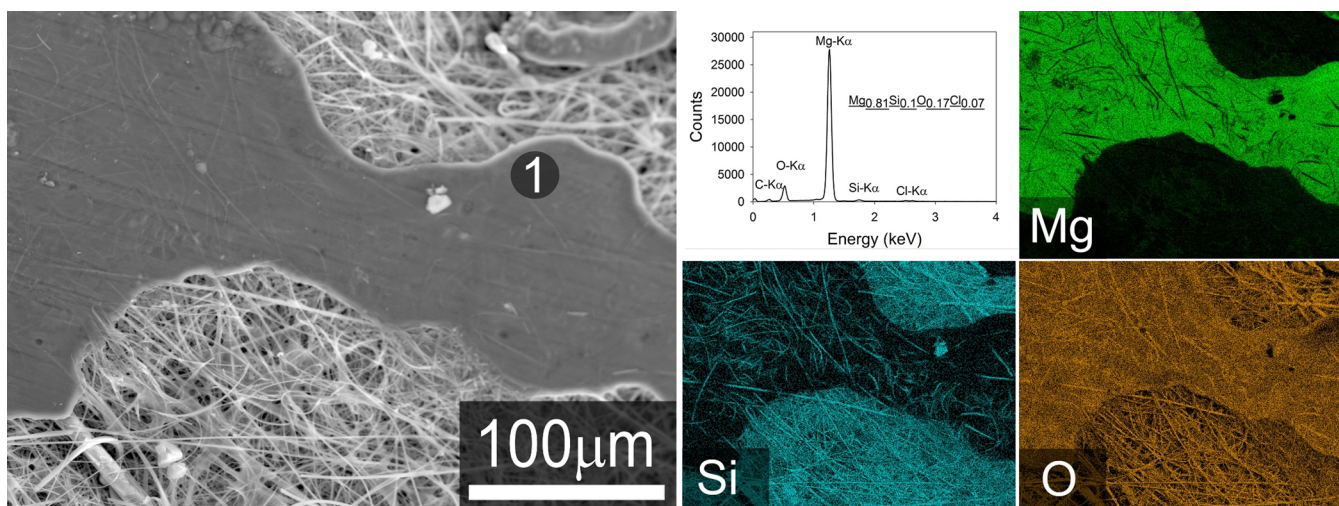
Figure 2. SEM image with associated EDS maps of the electrodeposited Mg on a Mo working electrode in the 1:2 $Mg[(DIPA)_2]$-$[C_2mim][AlCl_4]$. (Mg electrodeposits shown in the image are attached to the glass fiber separator during disassembly of the cell.)

shown in the inset of Figure 1d. While a significantly low CE is observed for all the working electrodes during the first cycles, the CE drastically improved with each cycle, ultimately reaching values of 78, 92, and 92%, respectively for the graphite foil, SS, and Mo at the 100th cycle. The CE of the Mo and SS working electrodes stabilizes in the range of 95−98% at the end of 500 cycles, suggesting decomposition of some of the electrolyte components and impurities accompanying the Mg^{2+} reduction for the nonunity CE. Such improvement in the overpotential and CE during reversible electrochemical cycling is a known phenomenon in electrolytes containing magnesium aluminum chloride, magnesium bis(trifluoromethylsulfonyl)-imide, and $Mg(TFSI)_2$-glyme complexes and is related to the removal of water during cycling.[33,58] Besides, a significantly lower CE for the graphite foil is not understood. The complexity involving the interactions between the graphite electrode surface and the electrolyte and the critical role played by even a trace amount of water impurity (<3 ppm) on altering the double-layer structure could play a significant role in determining Mg reversibility.[59,60] Mo exhibits the highest Mg deposition and stripping current density compared to graphite foil and SS. SEM-EDS and XRD results (Figure 2 and Figure S6, respectively) confirm the deposition of metallic Mg electrodeposited on a Mo working electrode at a current density of 0.5 mA cm^{-2} for 1 h.

Figure 3a shows the oxidative stability of the electrolyte using different working electrodes examined through LSV in the potential range of 2.0−5.0 V versus (Mg/Mg^{2+}). For comparison, LSV measurements are also carried out using a Pt working electrode under the same conditions. No marked increase in the current up to about 3.0 V manifests that the electrolyte, in general, has high intrinsic anodic stability and excellent compatibility with different working electrodes. The onset of the electro-oxidation process is advanced for the graphite foil and Pt with the anodic current beginning to surge as early as 3.0 V, which could be due to the catalytic reactions on the surface of these electrodes that oxidize trace impurities including water from the electrolyte. Similarly, a small increase in the oxidation current is observed on the SS and Mo electrodes at about 3.0 V, suggesting the formation of a passivation layer on the SS and Mo electrode surface. However, the steep rise in the anodic current is significantly
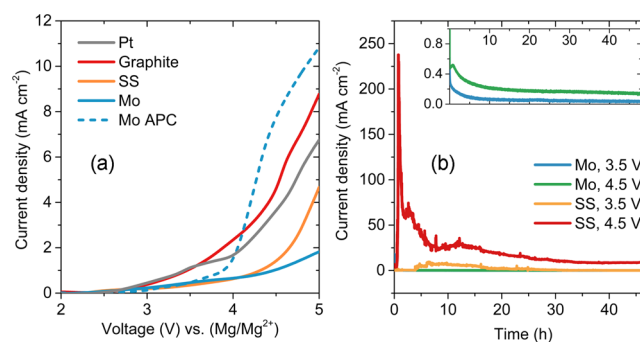

Figure 3. (a) Anodic LSVs using the 1:2 $Mg[(DIPA)_2]$-$[C_2mim]$-$[AlCl_4]$ electrolyte with different working electrodes recorded at a 20 mV s^{-1} scan rate (LSV of the state-of-the-art APC electrolyte with a Mo working electrode is included for comparison). (b) Chronoamperometry measurements for the Mo and SS working electrodes using 1:2 $Mg[(DIPA)_2]$-$[C_2mim][AlCl_4]$ electrolyte at 3.5 and 4.5 V vs (Mg/Mg^{2+})

delayed on these working electrodes. No appreciable increase in the oxidation current corresponding to the electrolyte or electrode degradation is noticed up to 4.3 V for both SS and Mo. Importantly, for Mo, the increase in the anodic current is considerably suppressed even up to 5.0 V. In comparison, the anodic stability of the state-of-the-art all phenyl complex (APC) electrolyte measured using the Mo working electrode is inferior, and the degradation starts at 3.6 V.

Chronoamperometry measurements carried out at potentials of 3.5 V and 4.5 V versus (Mg/Mg^{2+}) for 48 h to study the oxidation stability of the electrolyte with SS and Mo working electrodes are shown in Figure 3b. Although a mild but notable evolution of oxidation currents is observed for the SS working electrode while holding at 3.5 V, large oxidation currents are eventually obtained at 4.5 V. SEM micrographs (Figure 4a−c) of SS current collectors before and after stability testing at 3.5 V are shown, and 4.5 V provides clear evidence of corrosion, with high levels of pitting evident. Under testing at 3.5 V, the tested SS initially appears stable, thus complementing the results from LSV measurements shown in Figure 3a.

Nevertheless, an increase in the oxidation current is observed to occur after around 4 h, suggesting that the corrosion of SS occurs over time. Interestingly, the high
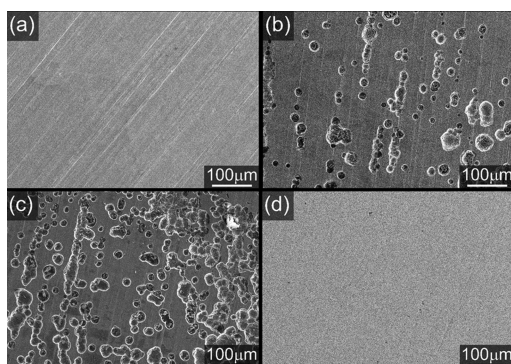
Figure 4. Secondary electron micrographs of SS316 (a) polished, (b) after 48 h hold at 3.5 V, (c) after 48 h hold at 4.5 V. Molybdenum after 48 h hold at 4.5 V is given in (d)

magnification image of the corrosion (Figure S7) shows morphology more consistent with grain boundary (intergranular) corrosion than with bulk corrosion, which may suggest a route to stable SS substrates via control of grain boundary composition. Nevertheless, comparison with the literature suggests that the SS tested here appears more stable to corrosion with the IL-based electrolyte reported in this work than a similar material tested with APC and $(HMDS)_2Mg$-$AlCl_3$/tetraglyme.[61]

In contrast, the oxidation currents from the Mo working electrodes are very low at both the potentials due to the formation of stable passivation layers on the Mo substrate. SEM micrographs taken after the potential hold test at 4.5 V confirm this, with no detectable corrosion being observed (Figure 4d). These results correlate well with the report that Mo develops stable passive films in chloride-containing

electrolytes such as APC.[62] The non-nucleophilic nature of the ILs employed in this work is considered to provide a less corrosive environment to Mo and SS current collectors, thus significantly enhancing their anodic stability.

Figure 5a shows the performance of the 1:2 $Mg[(DIPA)_2]$-$[C_2mim][AlCl_4]$ electrolyte for reversible Mg intercalation and extraction investigated by CV analysis with a Chevrel phase Mo_6S_8 cathode on a Mo current collector. The CV profiles indicate that the electrolyte facilitates the Mg intercalation/ extraction process with a high level of reversibility for at least 100 CV cycles. As reported in the literature, a two-step Mg intercalation process in Mo_6S_8 is observed, indicating the sequential formation of $MgMo_6S_8$ and $Mg_2Mo_6S_8$ (Figure 5a, inset).[63,64] However, as observed from the figure, distinguishing between the two cathodic peaks is not straightforward due to overlap.

The full cell performance of the electrolyte is investigated galvanostatically at 15 and 30 mA g^{-1} with a Mo_6S_8 cathode on a graphite foil and Mo current collector. According to Figure 5b, Mo_6S_8 exhibits better rate capability with a Mo current collector than with a graphite foil. Since the electrode materials and the electrolyte are the same in both the measurements, the electrochemical processes at the electrode/electrolyte interface are assumed to be identical. Therefore, the difference in the rate performance could have resulted from the inherent properties of the current collector and the nature of the cathode/current collector interface. Being metal, the electrical conductivity of Mo (1.9×10^7 S m^{-1}) is significantly higher than graphite (3.3×10^2–2.5×10^5 S m^{-1}). Also, the interfacial resistance resulting from the surface oxides on the current collectors, wettability, and poor adhesion of the active layer could affect the cell performance at high C-rates.
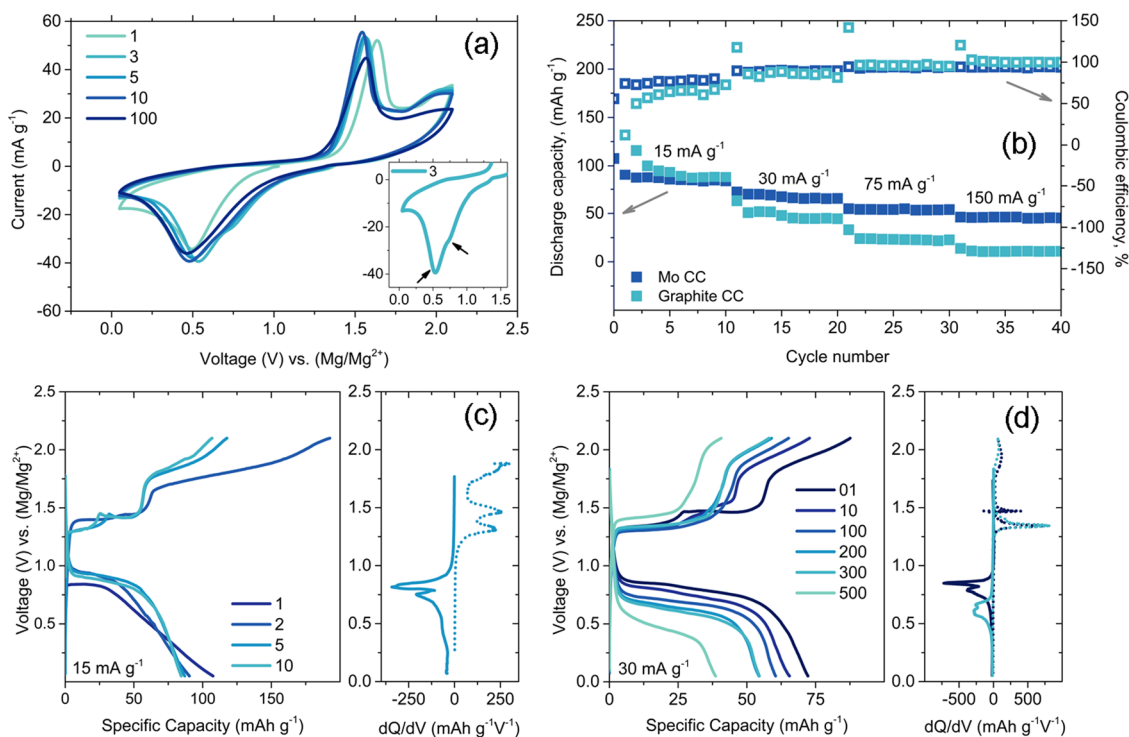
Figure 5. (a) CV curves of Mg-ion full cell with Mo_6S_8 cathode in 1:2 $Mg[(DIPA)_2]$- $[C_2mim][AlCl_4]$ electrolyte at a scan rate of 0.2 mV s^{-1}. (b) Rate performance with a Mo_6S_8 cathode in 1:2 $Mg[(DIPA)_2]$-$[C_2mim][AlCl_4]$ electrolyte (c) Galvanostatic charge−discharge performance at 15 mA g^{-1} and the associated dQ/dV curves. (d) Long-term cycling performance at 30 mA g^{-1} and the associated dQ/dV curves
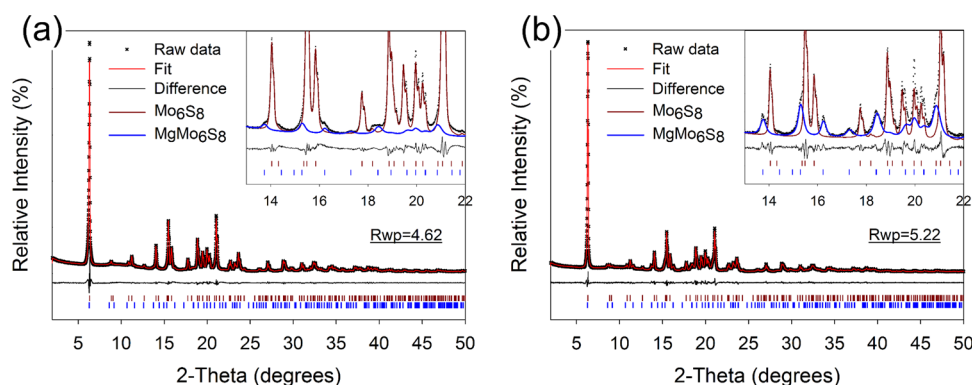
Figure 6. XRD patterns of the Mo_6S_8 cathode measured (a) after the first discharge cycle and (b) after the first charge cycle

Figure 5c shows selected charge/discharge profiles of the Mg-ion cell from the first 10 cycles at 15 mA g^{-1}. The plateau potential of the first discharge is found to be slightly lower than for the subsequent cycles, suggesting improved kinetics after the first cycle. At the end of the first discharge, a specific capacity of 110 mA g^{-1} is achieved against the theoretical value of 128 mA g^{-1} for the Mo_6S_8 cathode. After the first discharge/charge cycle, the cell performance is found to be stable, and at the end of 10 cycles, the cathode is able to provide a specific capacity of 85 mA g^{-1}, which is consistent with the values reported in the literature under similar currents.[50,65]

Structural analysis of the Mo_6S_8 cathode is performed after the first discharge and after the first charge step, using XRD to understand the reversibility of the Mg intercalation/extraction process during cycling (Figure 6a,b). The XRD pattern of the Mo_6S_8 cathode after Mg^{2+} insertion during the first discharge process exhibits two phases, the host Mo_6S_8 phase and a newly formed $MgMo_6S_8$ phase. Mg^{2+} intercalation (and extraction) into Mo_6S_8 occurs in two stages, and the differential capacity (dQ/dV) plotted as a function of voltage (Figure 5c) confirms the presence of two magnesiation and two demagnesiation processes occurring in the Mo_6S_8 cathode. However, it is essential to note that the XRD analysis does not verify the second $Mg_2Mo_6S_8$ phase. $Mg_2Mo_6S_8$ phase is generally considered to be unstable when exposed to air.[66,67] Once exposed (in this case for XRD analysis), $Mg_2Mo_6S_8$ would react with oxygen steadily, resulting in the extraction of Mg^{2+} from this phase, and this could be the reason that this phase is not observed in the XRD studies.

The XRD pattern of the Mo_6S_8 cathode after a fully charged state shows that Mo_6S_8 is the dominant phase, and it is an indication that the Mg^{2+} insertion/extraction process is reversible. However, the figure shows that complete reversibility is not achieved, and a trace amount of $MgMo_6S_8$ is still observed after the extraction process. This behavior of partial Mg^{2+} trapping in the host Mo_6S_8 during extraction at room temperature is reported in detail in the literature.[67] This partial entrapment of Mg^{2+} during the first charge step results in the drop in cell capacity, in this work from 110 to 90 mAh g^{-1}. The inability to completely extract Mg^{2+} is a drawback, as this cathode cannot be fully utilized, resulting in a lower practical, specific energy.

The cyclic stability and the associated charge/discharge curves of the Mg-ion cell cycled at a current rate of 30 mA g^{-1} shown in Figures 5d and 7, indicate that the IL-based electrolyte can support the reversible electrochemical processes over a long period. According to the figures, a noticeable drop
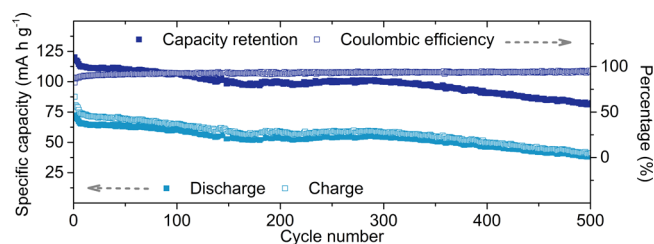

Figure 7. Cyclic stability, capacity retention, and Coulombic efficiency of Mg-ion full cell charged and discharged at 30 mA g^{-1} with the Mo_6S_8 cathode in the 1:2 $Mg[(DIPA)_2]$-$[C_2mim][AlCl_4]$ electrolyte

in the discharge performance (from 74 to 68 mAh g^{-1}) is observed during the first 10 cycles. After the initial performance loss, the cell is able to perform for hundreds of cycles with a nominal loss in capacity and with a CE of 93%. Above all, if normalized with the discharge capacity obtained at the end of the formation cycles (first 10 cycles), the cell is found to cycle for about 335 cycles with less than 20% loss in the initial capacity.

To demonstrate the applicability of the proposed electrolyte with high voltage cathodes, full cell cycling tests are conducted using V_2O_5 as the cathode material, and the results are collected in Figure S8. Besides, the charge/discharge profile of the V_2O_5 cathode cycled with the APC electrolyte is included in the figure for comparison. A significant improvement in the charge/discharge performance is observed with the V_2O_5 cathode when using the 1:2 $Mg[(DIPA)_2]$ and $[C_2mim]$-$[AlCl_4]$ electrolyte, validating the suitability of the IL-based electrolyte with high-voltage cathode materials. Notably, the charging voltage could be pushed to >3.5 V with the IL-based electrolyte enabled by the electrolyte's superior anodic stability. A specific capacity of about 70 mAh g^{-1} is obtained from the first discharge, which is similar to what is reported in the literature.[68] On the downside, the cathode material exhibited a short cycle life, and understanding the failure mechanisms is a subject for further research. In short, the half cell and full cell results obtained in this work demonstrate that by providing high anodic stability and cycle life, the new IL-based electrolyte reported here would be an excellent candidate for high-voltage rechargeable Mg-ion batteries.

4. CONCLUSIONS

In this work, we have developed a novel non-nucleophilic IL-based electrolyte containing $Mg[(DIPA)_2]$ and $[C_2mim]$-$[AlCl_4]$ in 1:2 molar ratio for rechargeable Mg-ion batteries.

The electrolyte shows superior performance in terms of reversibility and CE for the Mg deposition/stripping process. In combination with Mo as the working electrode (cathode current collector), the electrolyte is found to be electrochemically stable up to at least 4.5 V, and no corrosion of Mo is found even after holding it at 4.5 V for 48 h. A lifetime of over 300 cycles with >80% capacity retention is achieved in the full cell test with a Mo_6S_8 cathode. Besides, as the proof of concept, the electrolyte is also proven to work with a high-voltage V_2O_5 cathode. The straight forward, easy, and scalable synthesis method of the new electrolyte in combination with its excellent half-cell properties and full cell performance with prototype Mo_6S_8 and V_2O_5 cathodes make this electrolyte an excellent candidate for rechargeable Mg batteries.

■ ASSOCIATED CONTENT

ⓢ Supporting Information

The Supporting Information is available free of charge at https://pubs.acs.org/doi/10.1021/acsaem.0c01026.

> ESI-MS and Raman spectra of the electrolyte, electrochemical performance of the electrolyte in half-cells, XRD of the electrodeposited Mg, SEM of the corroded SS working electrode, charge/discharge cycles of the Mg/V_2O_5 full cell, and XRD and SEM of V_2O_5 (PDF)

■ AUTHOR INFORMATION

Corresponding Authors

Lethesh Kallidanthiyil Chellappan − *Department of Chemistry, Norwegian University of Science and Technology (NTNU), Trondheim 7491, Norway;* Email: lethesh.k.chellappan@ntnu.no

Kaushik Jayasayee − *New Energy Solutions, SINTEF Industry, Trondheim 7034, Norway;* ⓞ orcid.org/0000-0001-5532-5636; Email: kaushik.jayasayee@sintef.no

Authors

Jannicke Kvello − *New Energy Solutions, SINTEF Industry, Trondheim 7034, Norway*

Julian Richard Tolchard − *New Energy Solutions, SINTEF Industry, Trondheim 7034, Norway*

Paul Inge Dahl − *New Energy Solutions, SINTEF Industry, Trondheim 7034, Norway*

Sidsel Meli Hanetho − *New Energy Solutions, SINTEF Industry, Trondheim 7034, Norway*

Romain Berthelot − *ICGM, University of Montpellier, CNRS, Montpellier 34090, France; Réseau sur le Stockage Electrochimique de l'Energie (RS2E), CNRS, Amiens 80039, France*

Anne Fiksdahl − *Department of Chemistry, Norwegian University of Science and Technology (NTNU), Trondheim 7491, Norway*

Complete contact information is available at:
https://pubs.acs.org/10.1021/acsaem.0c01026

Notes

The authors declare no competing financial interest.

■ ACKNOWLEDGMENTS

■ REFERENCES

(1) Goodenough, J. B.; Park, K.-S. The Li-ion rechargeable battery: a perspective. *J. Am. Chem. Soc.* **2013**, *135*, 1167−1176.

(2) Hassoun, J.; Lee, K.-S.; Sun, Y.-K.; Scrosati, B. An advanced lithium ion battery based on high performance electrode materials. *J. Am. Chem. Soc.* **2011**, *133*, 3139−3143.

(3) Pan, B.; Zhang, J.; Huang, J.; Vaughey, J. T.; Zhang, L.; Han, S.-D.; Burrell, A. K.; Zhang, Z.; Liao, C. A Lewis acid-free and phenolate-based magnesium electrolyte for rechargeable magnesium batteries. *Chem. Commun.* **2015**, *51*, 6214−6217.

(4) Liao, C.; Sa, N.; Key, B.; Burrell, A. K.; Cheng, L.; Curtiss, L. A.; Vaughey, J. T.; Woo, J.-J.; Hu, L.; Pan, B.; Zhang, Z. The unexpected discovery of the Mg (HMDS) 2/MgCl 2 complex as a magnesium electrolyte for rechargeable magnesium batteries. *J. Mater. Chem. A* **2015**, *3*, 6082−6087.

(5) Yoshio, M.; Brodd, R. J.; Kozawa, A. *Lithium-ion batteries*; Springer: 2009; Vol. 1.

(6) Jaguemont, J.; Boulon, L.; Dubé, Y. A comprehensive review of lithium-ion batteries used in hybrid and electric vehicles at cold temperatures. *Appl. Energy* **2016**, *164*, 99−114.

(7) Yoo, H. D.; Shterenberg, I.; Gofer, Y.; Gershinsky, G.; Pour, N.; Aurbach, D. Mg rechargeable batteries: an on-going challenge. *Energy Environ. Sci.* **2013**, *6*, 2265−2279.

(8) Jayasayee, K.; Berthelot, R.; Lethesh, K.; Sheridan, E. Anode Materials for Rechargeable Mg Batteries. In *Magnesium Batteries*; Royal Society of Chemistry 2019; pp. 114−141.

(9) Saha, P.; Datta, M. K.; Velikokhatnyi, O. I.; Manivannan, A.; Alman, D.; Kumta, P. N. Rechargeable magnesium battery: Current status and key challenges for the future. *Prog. Mater. Sci.* **2014**, *66*, 1−86.

(10) Muldoon, J.; Bucur, C. B.; Oliver, A. G.; Sugimoto, T.; Matsui, M.; Kim, H. S.; Allred, G. D.; Zajicek, J.; Kotani, Y. Electrolyte roadblocks to a magnesium rechargeable battery. *Energy Environ. Sci.* **2012**, *5*, 5941−5950.

(11) Gaddum, L. W.; French, H. E. The electrolysis of grignard solutions1. *J. Am. Chem. Soc.* **1927**, *49*, 1295−1299.

(12) Shterenberg, I.; Salama, M.; Gofer, Y.; Levi, E.; Aurbach, D. The challenge of developing rechargeable magnesium batteries. *MRS Bull.* **2014**, *39*, 453−460.

(13) Yagi, S.; Tanaka, A.; Ichikawa, Y.; Ichitsubo, T.; Matsubara, E. Electrochemical stability of magnesium battery current collectors in a grignard reagent-based electrolyte. *J. Electrochem. Soc.* **2013**, *160*, C83.

(14) Gregory, T. D.; Hoffman, R. J.; Winterton, R. C. Nonaqueous Electrochemistry of Magnesium. *J. Electrochem. Soc.* **1990**, *137*, 775.

(15) Aurbach, D.; Lu, Z.; Schechter, A.; Gofer, Y.; Gizbar, H.; Turgeman, R.; Cohen, Y.; Moshkovich, M.; Levi, E. Prototype systems for rechargeable magnesium batteries. *Nature* **2000**, *407*, 724−727.

(16) Pour, N.; Gofer, Y.; Major, D. T.; Aurbach, D. Structural Analysis of Electrolyte Solutions for Rechargeable Mg Batteries by Stereoscopic Means and DFT Calculations. *J. Am. Chem. Soc.* **2011**, *133*, 6270−6278.

(17) Mohtadi, R.; Mizuno, F. Magnesium batteries: Current state of the art, issues and future perspectives. *Beilstein J. Nanotechnol.* **2014**, *5*, 1291−1311.

(18) Doe, R. E.; Han, R.; Hwang, J.; Gmitter, A. J.; Shterenberg, I.; Yoo, H. D.; Pour, N.; Aurbach, D. Novel, electrolyte solutions comprising fully inorganic salts with high anodic stability for rechargeable magnesium batteries. *Chem. Commun.* **2014**, *50*, 243−245.

(19) Kim, H. S.; Arthur, T. S.; Allred, G. D.; Zajicek, J.; Newman, J. G.; Rodnyansky, A. E.; Oliver, A. G.; Boggess, W. C.; Muldoon, J. Structure and compatibility of a magnesium electrolyte with a sulphur cathode. *Nat. Commun.* **2011**, *2*, 427.

(20) Wang, F.-f.; Guo, Y.-s.; Yang, J.; Nuli, Y.; Hirano, S.-i. A novel electrolyte system without a Grignard reagent for rechargeable magnesium batteries. *Chem. Commun.* **2012**, *48*, 10763−10765.

(21) Guo, Y.-s.; Zhang, F.; Yang, J.; Wang, F.-f.; NuLi, Y.; Hirano, S.-i. Boron-based electrolyte solutions with wide electrochemical

windows for rechargeable magnesium batteries. *Energy Environ. Sci.* **2012**, *5*, 9100−9106.

(22) Zhao-Karger, Z.; Zhao, X.; Wang, D.; Diemant, T.; Behm, R. J.; Fichtner, M. Performance Improvement of Magnesium Sulfur Batteries with Modified Non-Nucleophilic Electrolytes. *Adv. Energy Mater.* **2015**, *5*, 1401155.

(23) Vinayan, B. P.; Zhao-Karger, Z.; Diemant, T.; Chakravadhanula, V. S. K.; Schwarzburger, N. I.; Cambaz, M. A.; Behm, R. J.; Kübel, C.; Fichtner, M. Performance study of magnesium−sulfur battery using a graphene based sulfur composite cathode electrode and a non-nucleophilic Mg electrolyte. *Nanoscale* **2016**, *8*, 3296−3306.

(24) Yu, X.; Manthiram, A. Performance enhancement and mechanistic studies of magnesium−sulfur cells with an advanced cathode structure. *ACS Energy Lett.* **2016**, *1*, 431−437.

(25) Du, A.; Zhang, Z.; Qu, H.; Cui, Z.; Qiao, L.; Wang, L.; Chai, J.; Lu, T.; Dong, S.; Dong, T.; Xu, H.; Zhou, X.; Cui, G. An efficient organic magnesium borate-based electrolyte with non-nucleophilic characteristics for magnesium−sulfur battery. *Energy Environ. Sci.* **2017**, *10*, 2616−2625.

(26) Zhang, Z.; Cui, Z.; Qiao, L.; Guan, J.; Xu, H.; Wang, X.; Hu, P.; Du, H.; Li, S.; Zhou, X.; Dong, S.; Liu, Z.; Cui, G.; Chen, L. Novel Design Concepts of Efficient Mg-Ion Electrolytes toward High-Performance Magnesium−Selenium and Magnesium−Sulfur Batteries. *Adv. Energy Mater.* **2017**, *7*, 1602055.

(27) Xu, H.; Zhang, Z.; Cui, Z.; Du, A.; Lu, C.; Dong, S.; Ma, J.; Zhou, X.; Cui, G. Strong anion receptor-assisted boron-based Mg electrolyte with wide electrochemical window and non-nucleophilic characteristic. *Electrochem. Commun.* **2017**, *83*, 72−76.

(28) Mohtadi, R.; Matsui, M.; Arthur, T. S.; Hwang, S.-J. Magnesium Borohydride: From Hydrogen Storage to Magnesium Battery. *Angew. Chem. Int. Ed.* **2012**, *51*, 9780−9783.

(29) Tutusaus, O.; Mohtadi, R.; Arthur, T. S.; Mizuno, F.; Nelson, E. G.; Sevryugina, Y. V. An Efficient Halogen-Free Electrolyte for Use in Rechargeable Magnesium Batteries. *Angew. Chem. Int. Ed.* **2015**, *54*, 7900−7904.

(30) Herb, J. T.; Nist-Lund, C. A.; Arnold, C. B. A Fluorinated Alkoxyaluminate Electrolyte for Magnesium-Ion Batteries. *ACS Energy Lett.* **2016**, *1*, 1227−1232.

(31) Herb, J. T.; Nist-Lund, C. A.; Arnold, C. B. A fluorinated dialkoxide-based magnesium-ion electrolyte. *J. Mater. Chem. A* **2017**, *5*, 7801−7805.

(32) Liu, T.; Shao, Y.; Li, G.; Gu, M.; Hu, J.; Xu, S.; Nie, Z.; Chen, X.; Wang, C.; Liu, J. A facile approach using MgCl 2 to formulate high performance Mg 2+ electrolytes for rechargeable Mg batteries. *J. Mater. Chem. A* **2014**, *2*, 3430−3438.

(33) Barile, C. J.; Barile, E. C.; Zavadil, K. R.; Nuzzo, R. G.; Gewirth, A. A. Electrolytic conditioning of a magnesium aluminum chloride complex for reversible magnesium deposition. *J. Phys. Chem. C* **2014**, *118*, 27623−27630.

(34) Barile, C. J.; Spatney, R.; Zavadil, K. R.; Gewirth, A. A. Investigating the reversibility of in situ generated magnesium organohaloaluminates for magnesium deposition and dissolution. *J. Phys. Chem. C* **2014**, *118*, 10694−10699.

(35) Attias, R.; Salama, M.; Hirsch, B.; Goffer, Y.; Aurbach, D. Anode-Electrolyte Interfaces in Secondary Magnesium Batteries. *Joule* **2019**, *3*, 27−52.

(36) Ma, Z.; MacFarlane, D. R.; Kar, M. Mg Cathode Materials and Electrolytes for Rechargeable Mg Batteries: A Review. *Batteries Supercaps* **2019**, *2*, 115−127.

(37) Ha, S.-Y.; Lee, Y.-W.; Woo, S. W.; Koo, B.; Kim, J.-S.; Cho, J.; Lee, K. T.; Choi, N.-S. Magnesium (II) bis (trifluoromethane sulfonyl) imide-based electrolytes with wide electrochemical windows for rechargeable magnesium batteries. *ACS Appl. Mater. Interfaces* **2014**, *6*, 4063−4073.

(38) Wang, P.; NuLi, Y.; Yang, J.; Feng, Z. Mixed ionic liquids as electrolyte for reversible deposition and dissolution of magnesium. *Surf. Coat. Technol.* **2006**, *201*, 3783−3787.

(39) Su, S.; NuLi, Y.; Wang, N.; Yusipu, D.; Yang, J.; Wang, J. Magnesium Borohydride-Based Electrolytes Containing 1-butyl-1-methylpiperidinium bis (trifluoromethyl sulfonyl) imide Ionic Liquid for Rechargeable Magnesium Batteries. *J. Electrochem. Soc.* **2016**, *163*, D682−D688.

(40) NuLi, Y.; Yang, J.; Wu, R. Reversible deposition and dissolution of magnesium from BMIMBF4 ionic liquid. *Electrochem. Commun.* **2005**, *7*, 1105−1110.

(41) Novák, P.; Imhof, R.; Haas, O. Magnesium insertion electrodes for rechargeable nonaqueous batteries—a competitive alternative to lithium? *Electrochim. Acta* **1999**, *45*, 351−367.

(42) Cheek, G. T.; O'Grady, W. E.; El Abedin, S. Z.; Moustafa, E. M.; Endres, F. Studies on the electrodeposition of magnesium in ionic liquids. *J. Electrochem. Soc.* **2008**, *155*, D91−D95.

(43) Kar, M.; Ma, Z.; Azofra, L. M.; Chen, K.; Forsyth, M.; MacFarlane, D. R. Ionic liquid electrolytes for reversible magnesium electrochemistry. *Chem. Commun.* **2016**, *52*, 4033−4036.

(44) Kar, M.; Tutusaus, O.; MacFarlane, D. R.; Mohtadi, R. Novel and versatile room temperature ionic liquids for energy storage. *Energy Environ. Sci.* **2018**, *12*, 566−571.

(45) Watkins, T.; Kumar, A.; Buttry, D. A. Designer ionic liquids for reversible electrochemical deposition/dissolution of magnesium. *J. Am. Chem. Soc.* **2016**, *138*, 641−650.

(46) Zhao, X.; Yang, Y.; NuLi, Y.; Li, D.; Wang, Y.; Xiang, X. A new class of electrolytes based on magnesium bis (diisopropyl) amide for magnesium−sulfur batteries. *Chem. Commun.* **2019**, *55*, 6086−6089.

(47) Fuller, J.; Carlin, R. T.; Osteryoung, R. A.; Koranaios, P.; Mantz, R. Anodization and Speciation of Magnesium in Chloride-Rich Room Temperature Ionic Liquids. *J. Electrochem. Soc.* **1998**, *145*, 24−28.

(48) Bertasi, F.; Hettige, C.; Sepehr, F.; Bogle, X.; Pagot, G.; Vezzù, K.; Negro, E.; Paddison, S. J.; Greenbaum, S. G.; Vittadello, M.; di Noto, V. A key concept in magnesium secondary battery electrolytes. *ChemSusChem* **2015**, *8*, 3069−3076.

(49) Lin, P.-C.; Sun, I.-W.; Chang, J.-K.; Su, C.-J.; Lin, J.-C. Corrosion characteristics of nickel, copper, and stainless steel in a Lewis neutral chloroaluminate ionic liquid. *Corros. Sci.* **2011**, *53*, 4318−4323.

(50) Zhao-Karger, Z.; Zhao, X.; Fuhr, O.; Fichtner, M. Bisamide based non-nucleophilic electrolytes for rechargeable magnesium batteries. *RSC Adv.* **2013**, *3*, 16330−16335.

(51) Keyzer, E. N.; Glass, H. F. J.; Liu, Z.; Bayley, P. M.; Dutton, S. E.; Grey, C. P.; Wright, D. S. Mg (PF6) 2-based electrolyte systems: understanding electrolyte−electrode interactions for the development of Mg-ion batteries. *J. Am. Chem. Soc.* **2016**, *138*, 8682−8685.

(52) Kang, S.-J.; Lim, S.-C.; Kim, H.; Heo, J. W.; Hwang, S.; Jang, M.; Yang, D.; Hong, S.-T.; Lee, H. Non-grignard and Lewis acid-free sulfone electrolytes for rechargeable magnesium batteries. *Chem. Mater.* **2017**, *29*, 3174−3180.

(53) Choi, S.-H.; Kim, J.-S.; Woo, S.-G.; Cho, W.; Choi, S. Y.; Choi, J.; Lee, K.-T.; Park, M.-S.; Kim, Y.-J. Role of Cu in Mo6S8 and Cu mixture cathodes for magnesium ion batteries. *ACS Appl. Mater. Interfaces* **2015**, *7*, 7016−7024.

(54) Liu, T.; Cox, J. T.; Hu, D.; Deng, X.; Hu, J.; Hu, M. Y.; Xiao, J.; Shao, Y.; Tang, K.; Liu, J. A fundamental study on the [(μ-Cl) 3 Mg 2 (THF) 6]+ dimer electrolytes for rechargeable Mg batteries. *Chem. Commun.* **2015**, *51*, 2312−2315.

(55) Plommer, H.; Murphy, J. N.; Dawe, L. N.; Kerton, F. M. Morpholine-Stabilized Cationic Aluminum Complexes and Their Reactivity in Ring-Opening Polymerization of ε-Caprolactone. *Inorg. Chem.* **2019**, *58*, 5253−5264.

(56) Angell, M.; Pan, C.-J.; Rong, Y.; Yuan, C.; Lin, M.-C.; Hwang, B.-J.; Dai, H. High Coulombic efficiency aluminum-ion battery using an AlCl3-urea ionic liquid analog electrolyte. *Proc. Natl. Acad. Sci.* **2017**, *114*, 834−839.

(57) Kiefer, J.; Fries, J.; Leipertz, A. Experimental vibrational study of imidazolium-based ionic liquids: Raman and infrared spectra of 1-ethyl-3-methylimidazolium bis (trifluoromethylsulfonyl) imide and 1-

ethyl-3-methylimidazolium ethylsulfate. *Appl. Spectrosc.* **2007**, *61*, 1306−1311.

(58) Fukutsuka, T.; Asaka, K.; Inoo, A.; Yasui, R.; Miyazaki, K.; Abe, T.; Nishio, K.; Uchimoto, Y. New Magnesium-ion Conductive Electrolyte Solution Based on Triglyme for Reversible Magnesium Metal Deposition and Dissolution at Ambient Temperature. *Chem. Lett.* **2014**, *43*, 1788−1790.

(59) Connell, J. G.; Genorio, B.; Lopes, P. P.; Strmcnik, D.; Stamenkovic, V. R.; Markovic, N. M. Tuning the Reversibility of Mg Anodes via Controlled Surface Passivation by H2O/Cl− in Organic Electrolytes. *Chem. Mater.* **2016**, *28*, 8268−8277.

(60) Merrill, L. C.; Schaefer, J. L. Conditioning-Free Electrolytes for Magnesium Batteries Using Sufone−Ether Mixtures with Increased Thermal Stability. *Chem. Mater.* **2018**, *30*, 3971−3974.

(61) Wall, C.; Zhao-Karger, Z.; Fichtner, M. Corrosion Resistance of Current Collector Materials in Bisamide Based Electrolyte for Magnesium Batteries. *ECS Electrochem. Lett.* **2014**, *4*, C8−C10.

(62) Cheng, Y.; Liu, T.; Shao, Y.; Engelhard, M. H.; Liu, J.; Li, G. Electrochemically stable cathode current collectors for rechargeable magnesium batteries. *J. Mater. Chem. A* **2014**, *2*, 2473−2477.

(63) Wan, L. F.; Perdue, B. R.; Apblett, C. A.; Prendergast, D. Mg desolvation and intercalation mechanism at the Mo6S8 chevrel phase surface. *Chem. Mater.* **2015**, *27*, 5932−5940.

(64) Cho, W.; Moon, B.; Woo, S. G.; Kim, J. H.; Park, M. S.; Kim, J. S.; Kim, H.; Kim, Y. J. Size effect of chevrel MgxMo6S8 as cathode material for magnesium rechargeable batteries. *Bull. Korean Chem. Soc.* **2015**, *36*, 1209−1214.

(65) Nelson, E. G.; Brody, S. I.; Kampf, J. W.; Bartlett, B. M. A magnesium tetraphenylaluminate battery electrolyte exhibits a wide electrochemical potential window and reduces stainless steel corrosion. *J. Mater. Chem. A* **2014**, *2*, 18194−18198.

(66) Lancry, E.; Levi, E.; Gofer, Y.; Levi, M.; Salitra, G.; Aurbach, D. Leaching chemistry and the performance of the Mo6S8 cathodes in rechargeable Mg batteries. *Chem. Mater.* **2004**, *16*, 2832−2838.

(67) Levi, E.; Lancry, E.; Mitelman, A.; Aurbach, D.; Ceder, G.; Morgan, D.; Isnard, O. Phase diagram of Mg insertion into chevrel phases, Mg x Mo6T8 (T= S, Se). 1. Crystal structure of the sulfides. *Chem. Mater.* **2006**, *18*, 5492−5503.

(68) Son, S.-B.; Gao, T.; Harvey, S. P.; Steirer, K. X.; Stokes, A.; Norman, A.; Wang, C.; Cresce, A.; Xu, K.; Ban, C. An artificial interphase enables reversible magnesium chemistry in carbonate electrolytes. *Nat. Chem.* **2018**, *10*, 532−539.